

# A tactile sensor capable of mechanical adaptation and its use as a surface deflection detector

Ryo Kikuuwe, Akihito Sano, Hiromi Mochiyama, Naoyuki Takesue, and Hideo Fujimoto  
*Touch Tech Lab Funded By Toyota, Nagoya Institute of Technology, Aichi 466-8555, Japan*  
kikuuwe@ieee.org

**Abstract**—This paper proposes a sensor mechanism that detects temporal changes in shear strain. It is composed of a deformable capsule, viscous fluid filled in the capsule, single or multiple cantilevers projecting into the capsule, and strain gage(s) attached to the cantilever(s). When the capsule is being deformed, the cantilever receives bending force from the fluid. The mechanical adaptation function prevents mechanical damage to the strain gages and the saturation of the signal. We intend to use this sensor to the sheet metal inspection process in the automobile industry to detect surface deflection defects on the metal surfaces.

## I. INTRODUCTION

In the automobile industry, the pressed metal sheets are inspected to detect small deflection defects. This inspection process has been performed by well-trained craftsworker's touch. Automatic measurement tools are difficult to be introduced in this process because they are generally inefficient and not robust. For example, laser displacement sensors and dial gages are sensitive to positioning errors and are not suitable for scanning a wide area in a short time. Image processing is sensitive to extraneous materials such as oil spots. Because the manual inspection task requires highly trained skill and long experience, efficient inspection technologies have been sought.

In another report [1], we have proposed a device, called a tactile contact lens, for assisting manual process of the sheet metal inspection. In order to move forward to quantification of this inspection process, we need a tactile sensor device that can substitute the craftsworker's touch. Because the sheet metals are usually smoothly curved, the sensor needs to have a flexibility to follow the surface curvature. Moreover, it should respond to deflections with relatively high spatial frequency (e.g., surface deflection defects) without responding to gradual curvatures.

Using strain gages can be one of the easiest methods for measuring the deformation [2], [3]. When this approach is applied to relatively soft materials, a wide measurement range is required to avoid the signal saturation, and this usually results in a low measurement resolution. This problem may be avoided by an automatic gain controller [4]. However, there remains another problem that the strain gages can be mechanically damaged under a large deformation. Shinoda et al. [5] proposed a mechanically robust strain sensor element that measures the acoustic resonance frequencies of the air in a cavity in the material. If this is used for detecting

small changes in the strain, the resolution of the frequency measurement must be very high.

This paper proposes a sensor mechanism that has the function of mechanical adaptation. The basic structure of the proposed mechanism is illustrated in Fig. 1(a). This is composed of a deformable capsule, viscous fluid filled in the capsule, a cantilever projecting into the capsule, and a strain gage attached to the cantilever. When the capsule is being deformed, as shown in Fig. 1(b), the cantilever is bent by the viscous force of the fluid, and this bending is measured by the strain gage. This mechanism does not respond to temporally constant strain; it responds only to temporal changes in the strain. Therefore, it is suitable for detecting small change in strain in deformable objects. Moreover, this adaptation function prevents mechanical damage to the strain gages. When this device is slid on an object surface, as shown in Fig. 2, the cantilever receives the bending force as the inclination of the surface changes.

The proposed mechanism can be seen as a mechanism for detecting temporal changes in shear strain. This is expected to be useful as tactile sensors to be embedded in the artificial skin of robots. In the human glabrous skin, there are mainly 4 types of mechanoreceptors. The Meissner corpuscle is known as a rapidly-adapting receptor, and it is theoretically suggested that it responds to shear strain [6]. The proposed sensor may play a role correspondent to the Meissner corpuscle.

## II. THE PROTOTYPE

### A. Overview

Fig. 3 shows a prototype of the proposed sensor mechanism. This is produced from a commercially available polypropylene container. The bottom of the container is replaced by a polyethylene terephthalate (PET) sheet (thickness 0.3 mm). A rubber sheet (thickness 10 mm) is placed between the sidewall of the container and the bottom sheet to prevent the leak of the fluid. Two PET cantilevers ( $20 \times 5 \times 0.3$  mm) are attached to the base sheet with a separation of 15 mm. Strain gages are attached to the cantilevers, and silicone oil (kinetic viscosity  $1 \times 10^5$  mm<sup>2</sup>/sec) is filled in the container. Partition boards are installed in the container in order to suppress unnecessary vibration and fluxion of the silicone oil. To facilitate a tight contact between the bottom sheet and the target surface, PET disks (diameter 6 mm, thickness 0.3 mm) are attached immediately below the cantilevers.

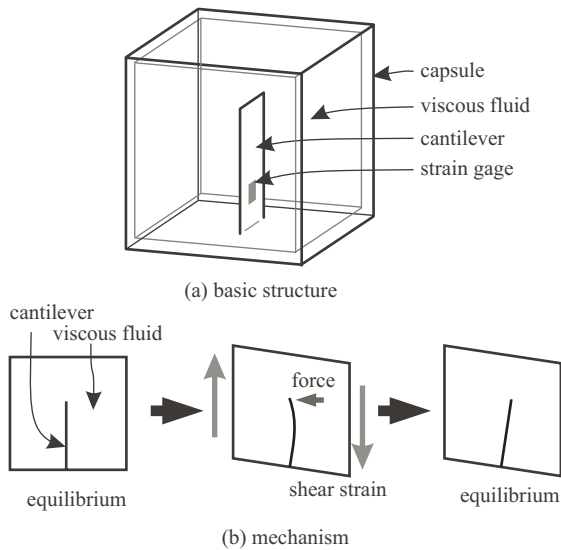


Fig. 1. The proposed sensor mechanism.

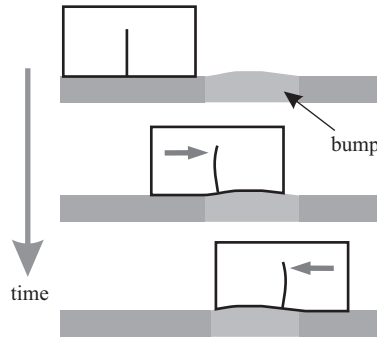
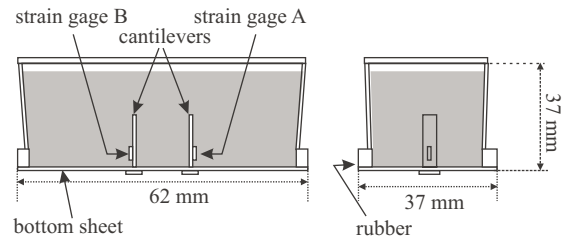


Fig. 2. Surface deflection detection using the proposed sensor.

### B. Algorithm for Detecting Surface Deflection

One problem with the proposed sensor is that this also responds to the acceleration applied to the whole device and the friction force applied to the bottom sheet. In the use as a surface deflection detector, the signal component resulting from surface deflections has to be isolated from those resulting from the acceleration and the friction force. One approach for this is to use data from multiple cantilevers. Signal components caused by the friction force and acceleration are simultaneously detected from the multiple cantilevers, but that caused by the surface deflection is detected with time differences among the multiple cantilevers. By using this method, we can selectively detect the signal caused by the surface deflection.

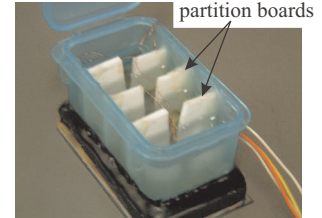
Now, we use Fig. 4 to explain the algorithm to detect the existence of a surface deflection by integrating signals from two adjacent cantilevers. Let  $a(t)$  denote the signal from Cantilever A at time  $t$ , and  $b(t)$  denote the signal from Cantilever B at time  $t$ . Fig. 4 shows the waveforms from two cantilevers when Cantilever A passed over a surface deflection through time  $t - c - h$  to time  $t - c$ , and subsequently Cantilever B passed over the same surface deflection through time  $t - h$  to time  $t$ .



(a) structure of the prototype (partition boards not shown)



(b) photograph of the prototype



(c) inside of the prototype

Fig. 3. A prototype of the proposed sensor mechanism.

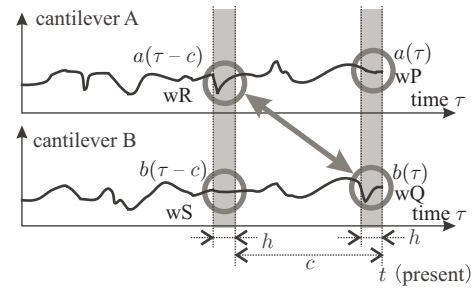


Fig. 4. Explanation of correlation computation.

Let us define 4 segments of waveforms:  $wP = \{a(\tau)\}_{t-h < \tau < t}$ ,  $wQ = \{b(\tau)\}_{t-h < \tau < t}$ ,  $wR = \{a(\tau - c)\}_{t-h < \tau < t}$ , and  $wS = \{b(\tau - c)\}_{t-h < \tau < t}$ . Then,  $wQ$  and  $wR$  are considered similar. In other words, we can judge that the cantilevers passed over a surface deflection in the order of A-B if  $wQ$  and  $wR$  are similar. The similarity between the two waveforms can be measured by the correlation coefficient.

We have to note that the similarity between the two waveforms can also be caused by a cyclic disturbance. If a cyclic disturbance exists,  $wQ$  becomes similar to  $wP$ ,  $wR$ , and  $wS$ . To evaluate the direct similarity between  $wQ$  and  $wR$  without intermediating  $wP$  and  $wS$ , we should use the

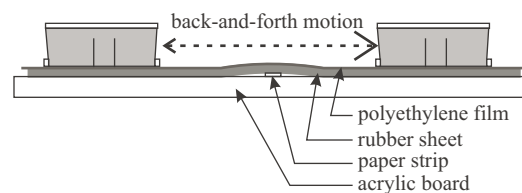


Fig. 5. Experimental procedure.

partial correlation coefficient instead of the total correlation coefficient.

Let us define the following vector:

$$\mathbf{u}(t, c) = [ a(t) , b(t) , a(t - c) , b(t - c) ]^T. \quad (1)$$

In the time segment  $t - h \leq \tau \leq t$ , the average and covariance matrix of  $\mathbf{u}(\tau, c)$  are respectively given as follows:

$$\bar{\mathbf{u}}(t, c) = \frac{1}{h} \int_{t-h}^t \mathbf{u}(\tau, c) d\tau \quad (2)$$

$$\begin{aligned} \mathbf{V}(t, c) &= \frac{1}{h} \int_{t-h}^t (\mathbf{u}(\tau, c) - \bar{\mathbf{u}}(t, c)) (\mathbf{u}(\tau, c) - \bar{\mathbf{u}}(t, c))^T d\tau \\ &= \frac{1}{h} \int_{t-h}^t \mathbf{u}(\tau, c) \mathbf{u}(\tau, c)^T d\tau - \bar{\mathbf{u}}(t, c) \bar{\mathbf{u}}(t, c)^T. \end{aligned} \quad (3)$$

Let  $\mathbf{U}(t, c) = \mathbf{V}(t, c)^{-1}$  and  $U_{ij}(t, c)$  denote  $\mathbf{U}(t, c)$ 's  $ij$ -th element. Then, the partial correlation of  $a(\tau - c)$  and  $b(\tau)$  with the effects of  $a(\tau)$  and  $b(\tau - c)$  removed is given as

$$R_{ab}(t, c) = \frac{-U_{23}(t, c)}{\sqrt{U_{22}(t, c)U_{33}(t, c)}}. \quad (4)$$

As well, the partial correlation of  $a(\tau)$  and  $b(\tau - c)$  with the effects of  $a(\tau - c)$  and  $b(\tau)$  removed is written as

$$R_{ba}(t, c) = \frac{-U_{14}(t, c)}{\sqrt{U_{11}(t, c)U_{44}(t, c)}}. \quad (5)$$

At time  $t$ , if there exists  $c$  for which  $R_{ab}(t, c)$  is close to 1, we can judge that the two cantilevers A and B passed over the surface deflection in the order A-B. As well, if there exists  $c$  for which  $R_{ba}(t, c)$  is close to 1, the cantilevers passed over the surface deflection in the order B-A. When the two strain gages are installed face-to-face as illustrated in Fig. 3, the signs of  $b(t)$  and  $b(t - c)$  in (1) have to be reversed.

In order to save the computational cost and the memory usage in the real-time calculation, the exponential weighting is preferable to the sliding-window approach described above. When the exponential weighting approach is used, (2) and (3) are respectively replaced by

$$\bar{\mathbf{u}}(t, c) = \int_0^t \frac{e^{-\frac{t-\tau}{\lambda}}}{\lambda} \mathbf{u}(\tau, c) d\tau \quad (6)$$

$$\mathbf{V}(t, c) = \int_0^t \frac{e^{-\frac{t-\tau}{\lambda}}}{\lambda} (\mathbf{u}(\tau, c) - \bar{\mathbf{u}}(t, c)) (\mathbf{u}(\tau, c) - \bar{\mathbf{u}}(t, c))^T d\tau. \quad (7)$$

Here,  $\lambda$  is a parameter that determines the decay speed of the weight (i.e., the speed of forgetting). The weight becomes  $1/e$  times after a time period  $\lambda$  elapses. The update rules of  $\bar{\mathbf{u}}(t, c)$  and  $\mathbf{V}(t, c)$  can be written as follows:

$$\bar{\mathbf{u}}(t, c) = r\bar{\mathbf{u}}(t - \Delta t, c) + (1 - r)\mathbf{u}(t, c) \quad (8)$$

$$\begin{aligned} \mathbf{S}(t, c) &= r\mathbf{S}(t - \Delta t, c) + (1 - r)\mathbf{u}(t, c)\mathbf{u}(t, c)^T \\ &\quad + (1 - r)\varepsilon^2 \mathbf{I}_4 \end{aligned} \quad (9)$$

$$\mathbf{V}(t, c) = \mathbf{S}(t, c) - \bar{\mathbf{u}}(t, c)\bar{\mathbf{u}}(t, c)^T. \quad (10)$$

Here,  $r = e^{-\Delta t/\lambda}$ ,  $\Delta t$  is the sampling interval,  $\mathbf{I}_4$  is the 4-by-4 unit matrix, and  $\varepsilon$  is a positive value that has the same physical dimension as  $a(t)$  and  $b(t)$ . The third term of the right-hand

side of (9) is for avoiding numerical instability when the magnitude of signal is very small. The initial values of  $\bar{\mathbf{u}}(t, c)$  and  $\mathbf{S}(t, c)$  are zero-vector and zero-matrix, respectively.

### C. Experiments

We performed simple experiments to validate the proposed sensor. The experimental condition was as illustrated in Fig. 3. A paper strip (width 5 mm, thickness 0.09 mm) was placed on an acrylic board, and it was hidden by a rubber sheet (thickness 5 mm) and a polyethylene film (thickness 0.06 mm). The bump on the polyethylene film produced by the paper strip was very gradual. This bump is difficult to be perceived by bare-handed touch, but can be perceived clearly with a tactile contact lens [1].

In the experiment, the prototype sensor was moderately pressed onto the experimental apparatus and moved back and forth by the experimenter's hand as illustrated in Fig. 5. The amplitude of the reciprocating movement was approximately 200 mm, and the frequency was approximately 0.5 Hz (slow movement) or 1 Hz (fast movement). The strain of the strain gages and the output of the detection algorithm were recorded. We recorded the data when the paper piece was present and when it was absent under with two movement speeds (slow and fast).

The sampling rate,  $\Delta t$ , is 2 msec, and  $c$  is chosen to be 2, 4,  $\dots$ , 150 msec. The value of  $\lambda$  is varied by  $c$  as  $\lambda = c$ . When there exists  $c$  for which  $R_{ab}(t, c)$  is larger than the threshold 0.85, we judge that the cantilevers are crossing over a deflection in the order of A-B. When there exists  $c$  for which  $R_{ba}(t, c)$  is larger than 0.85, we judge that the cantilevers are crossing over a deflection in the order of B-A. The values of  $a(t)$  and  $b(t)$  are substituted by the dimensionless values of the strain measured by the strain gages, and the constant  $\varepsilon$  is set to be  $7.0 \times 10^{-6}$ .

Fig. 6 shows the temporal profiles of the measurements of the strain gages A and B and the output of the detection algorithm. The output of the detection algorithm is 1 if there exists  $c$  for which  $R_{ab}(t, c) > 0.85$ ,  $-1$  if there exists  $c$  for which  $R_{ba}(t, c) > 0.85$ , or 0 otherwise.

In both cases of the slow movement and the fast movement, the presence of the deflection causes a distinct difference in the temporal profile of the strain (compare (a) to (b) and (c) to (d)). Moreover, the output values of the algorithm are correct in all cases. In the fast movement (Fig. 6(c)(d)), the acceleration at the velocity reversal appear to influence the raw data of measurement. However, the algorithm is shown to be capable of adequate detection.

### III. CONCLUSIONS

This paper has proposed a basic structure of a shear strain sensor having the function of mechanical adaptation. We have also proposed an algorithm for detecting small deflection of an object surface using the proposed sensor. The proposed sensor and the proposed algorithm were tested by simple experiments.

Future study should be directed to establish a design guideline of the sensor to optimize the dimensions of the cantilever,

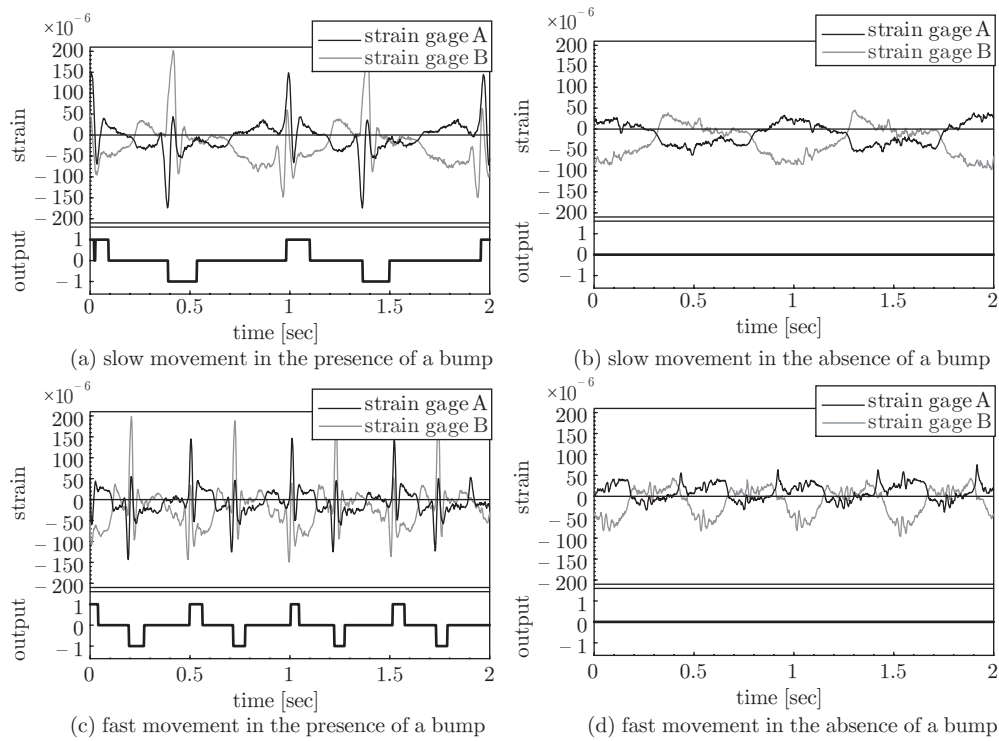


Fig. 6. Experimental results (the measurements of strain and the output of the proposed algorithm).

the stiffness of the cantilever, and the viscosity of the fluid. This will be necessary for downsizing of the device. Another remaining problem is the computational cost with the proposed algorithm. For practical application using inexpensive processors, more computationally efficient algorithm will be desirable. Moreover, we need to seek an improved structure of the sensor that is mechanically insensitive to the accelerations and the friction forces.

#### ACKNOWLEDGMENT

This work has been supported by Toyota Motor Corporation. We thank the engineers and craftsmen in Motomachi Plant of Toyota Motor Corporation who motivated and inspired our research.

#### REFERENCES

- [1] R. Kikuuwe, A. Sano, H. Mochiyama, N. Takesue, K. Tsunekawa, S. Suzuki and H. Fujimoto: "The tactile contact lens," Proceedings of the 3rd IEEE Conference on Sensors, 2004 (to appear).
- [2] D. Yamada, T. Maeno and Y. Yamada: "Artificial finger skin having ridges and distributed tactile sensors used for grasp force control," Journal of Robotics and Mechatronics, Vol. 14, No. 2, pp. 140-146, 2002.
- [3] Y. Tada, K. Hosoda, Y. Yamasaki and M. Asada: "Sensing the texture of surfaces by anthropomorphic soft fingertips with multi-modal sensors," Proceedings of the 2003 IEEE/RSJ International Conference on Intelligent Robots and Systems, pp.31-35, 2003.
- [4] M. Kaneko and R. Horie: "Tactile sensor with automatic gain control," Proceedings of the 2003 IEEE/RSJ International Conference on Intelligent Robots and Systems, pp.25-30, 2003.
- [5] H. Shinoda, K. Matsumoto and S. Ando: "Tactile sensing based on acoustic resonance tensor cell," Proceedings of the 9th International Conference on Solid-State Sensors and Actuators, pp.129-132, 1997.
- [6] T. Nara, M. Takasaki, T. Maeda, T. Higuchi, S. Ando and S. Tachi: "Surface acoustic wave tactile display," IEEE Computer Graphics and Applications, vol.21, no.6, pp.56-63, 2001.